第58卷 第3期
2020年7月

古 脊 椎 动 物 学 报
VERTEBRATA PALASIATICA

pp. 221–248
figs. 1–9

DOI: 10.19615/j.cnki.1000-3118.200320

New material of Cervidae (Artiodactyla, Mammalia) from Xinyaozi Ravine in Shanxi, North China

DONG Wei[1,2] BAI Wei-Peng[1,2,3] PAN Yue[1,2,3] LIU Wen-Hui[4]

(1 *Key Laboratory of Vertebrate Evolution and Human Origins of Chinese Academy of Sciences*, *Institute of Vertebrate Paleontology and Paleoanthropology*, *Chinese Academy of Sciences* Beijing 100044 dongwei@ivpp.ac.cn)
(2 *CAS Center for Excellence in Life and Paleoenvironment* Beijing 100044)
(3 *University of Chinese Academy of Sciences* Beijing 100049)
(4 *Institute of Environmental Archaeology*, *National Museum of China* Beijing 100006)

Abstract Many cervid specimens were uncovered during the field exploration for Nihewan beds at the beginning of the 1980s from Taijiaping, Shuichongkou and Dazhuangke localities along Xinyaozi Ravine at Nangaoya Township of Tianzhen County, Shanxi Province in North China. Recent studies on the cervid material identified seven species of Cervidae in total: *Muntiacus bohlini*, *Cervavitus* cf. *C. huadeensis*, *Axis shansius*, *Nipponicervus elegans*, *Elaphurus davidianus predavidianus*, *E. bifurcatus* from the Early Pleistocene deposits at Taijiaping and Shuichongkou localities, and *Cervus* (*Elaphus*) *elaphus* from uncertain horizon at Dazhuangke. At least the previous six species of cervids were from Nihewan Formation (Nihewanian or equivalent to European middle and late Villafranchian), i.e. the Early Pleistocene, in Sangganhe Basin area. *Cervavitus* cf. *C. huadeensis* and *A. shansius* were survivors from the Late Neogene; *M. bohlini*, *N. elegans*, *E. davidianus predavidianus* and *E. bifurcatus* are new forms of the Early Pleistocene. If Dazhuangke horizon can be dated as those of Shuichongkou and Taijiaping localities, the appearance of elaphoid cervids could be traced back to the Early Pleistocene, and the evolution of elaphoid antler would start from absence to presence of bez tine. The presence of *Elaphurus* and *Nipponicervus* in mainland China and Japanese archipelago implies further that the sea level was dropped down that these cervids could migrate from the mainland to the islands. The abundance of folivorous cervid specimens in the Xinyaozi Ravine area indicates the existence of a certain scale of forested environment in Sangganhe Basin area during the Early Pleistocene.

Key words Xinyaozi, Tianzhen, Shanxi, Sangganhe Basin, Nihewan Formation, middle and late Villafranchian, Early Pleistocene, Cervidae

Citation Dong W, Bai W P, Pan Y et al., 2020. New material of Cervidae (Artiodactyla, Mammalia) from Xinyaozi Ravine in Shanxi, North China. Vertebrata PalAsiatica, 58(3): 221–248

中国科学院战略性先导科技专项(B类) (编号：XDB 26030304)资助。
收稿日期：2019-12-12

1 Introduction

The field exploration for Nihewan beds at the beginning of the 1980s by the team of Wei Qi (1997) resulted in discovery of many cervid specimens from Taijiaping, Shuichongkou and Dazhuangke localities along Xinyaozi Ravine at Nangaoya Township of Tianzhen County, Shanxi Province in North China. The mammalian fossils collected along the ravine were called Xinyaozi fauna (Wei, 1997; Tong et al., 2011) and identified total four cervid taxa, i.e. *Muntiacus bohlini*, *Elaphurus bifurcatus*, *Eucladoceros boulei* and *Rusa elegans* (Wei, 1997). Although the localities are in Shanxi Province, they are very close to Xiashagou (=Hsia-sha-kou) localities (Teilhard de Chardin and Piveteau, 1930) in the Nihewan Basin yielding cervids such as *E. bifurcatus*, *Cervus* (*Rusa*) *elegance* etc. in Hebei Province. The fossils unearthed from the Shuichongkou deposits include *Nyctereutes* sp., *Canis* sp., *Agriotherium* sp., *Ursus* sp., *Meles* sp., *Felis* sp., *Pachycrocuta* sp., *Postschizotherium intermedium*, *Plesiohipparion houfenense*, *Equus sanmeniensis*, *Axis* sp. etc. (Qiu et al., 2002), as well as *Spirocerus wongi* (Bai et al., 2019). The faunal composition indicates an earlier age than that of the classical Nihewan fauna, likely ranging between 1.8 Ma and 2.6 Ma (Qiu et al., 2002). The fossils unearthed from Taijiaping deposits include *Canis chihliensis palmidens*, *Nyctereutes sinensis*, *Pachycrocuta licenti*, *Homotherium* sp., *Megantereon nihewanensis*, *Lynx* sp., *Felis* sp., *Proboscidipparion sinense*, *Equus sanmeniensis*, *Coelodonta yanshanensis*, ?*Rhinoceros* sp., *Gazella* sp., *Elaphurus bifurcatus* (Qiu, 2002), as well as *E. davidianus predavidianus* (Dong et al., 2019). The geologic age of the fauna can roughly be considered as contemporary with that of the classical Nihewan fauna (Qiu, 2002), with an estimated age of ca. 2.2–1.7 Ma (Liu et al., 2012), equivalent to from upper part of MNQ17 to lower part of NMQ18 (Woodburne, 2013). The deposits at Shuichongkou are therefore slightly earlier than those at Taijiaping. However, many specimens collected during the 1980s' explorations have not yet been systematically studied. We reinvestigated the localities along Xinyaozi Ravine in 2017, studied cervid specimens from Taijiaping locality and identified two *Elaphurus* species (Dong et al., 2019). Here we systematically describe the rest specimens of cervids from Xinyaozi Ravine at Tianzhen and discuss on their taxonomy and evolutionary history. The antler measurement methods follow that of Dong et al. (2019), the dental terminology follows that of Dong (2004). The complete skulls with both antlers and dentitions are unfortunately absent in the collection. The taxonomic assignment of the antlers, upper and lower dentitions were based on their relative dimensions and morphological comparison with available identified specimens. The specimens described are housed at the Institute of Vertebrate Paleontology and Paleoanthropology, Chinese Academy of Sciences (IVPP).

2 Systematic paleontology

Mammalia Linnaeus, 1758
Artiodactyla Owen, 1848

Ruminantia Scopoli, 1777
Pecora Flower, 1883
Cervoidea Simpson, 1931
Cervidae Gray, 1821
Muntiacinae Knottnerus-Meyer, 1907
***Muntiacus* Rafinesque, 1815**
***Muntiacus bohlini* (Teilhard de Chardin, 1940)**

(Figs. 1–2; Tables 1–3)

Cervulus cf. *sinensis* Teilhard de Chardin and Piveteau, 1930, p. 44–46
Cervulus bohlini sp. nov. Teilhard de Chardin, 1940, p. 79–88
Muntiacus bohlini Hooijer, 1951, p. 7
Muntiacus bohlini Wang and Wu, 1979, p. 541
Muntiacus bohlini Wei, 1997, p. 196

Material A nearly complete left antler with burr and broken pedicle (IVPP V 26267.1) from Shuichongkou; a right maxillary fragment with M1–3 (V 26267.2), a left mandibular fragment with p2–m2 (V 26267.3), a right mandibular fragment with p3–m3 (V 26267.4), and a right mandibular fragment with dp4–m2 (V 26267.5) from Taijiaping, Tianzhen, Shanxi.

Description The specimen V 26267.1 (Fig. 1) is a left mature but unshed antler (see Table 1 for measurements) from an adult individual. Its pedicle is broken but a small part remained just below the burr. The cross sections of the pedicle are oval and the surface of the

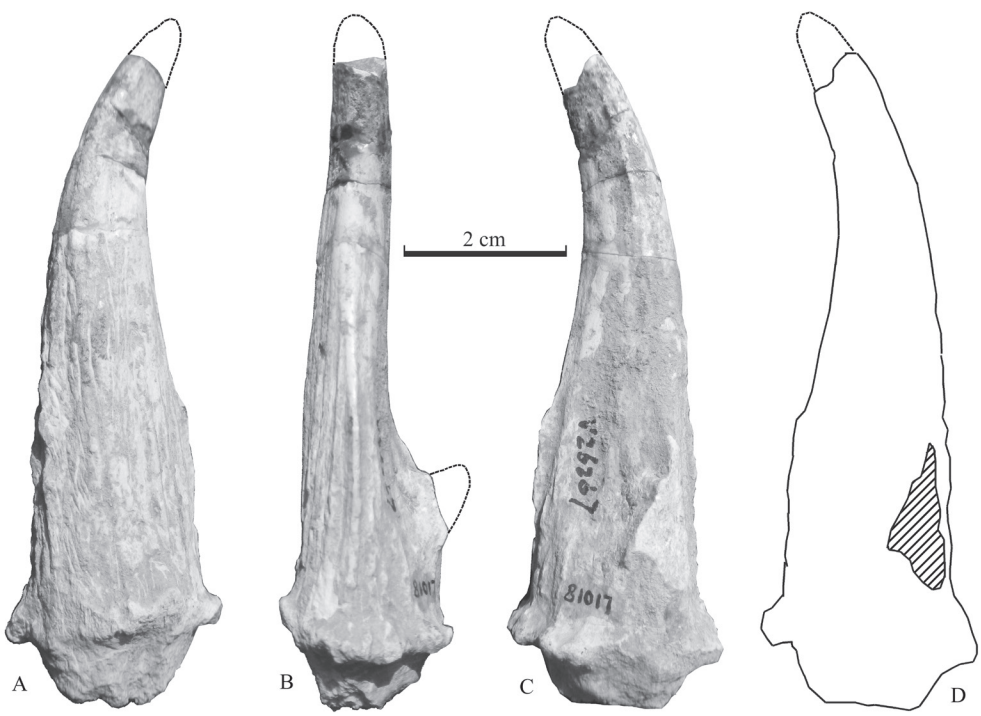

Fig. 1 A nearly complete antler (IVPP V 26267.1) of *Muntiacus bohlini* from Xinyaozi Ravine
A. lateral view; B. medial view; C. anterior-medial view; D. outline of anterior-medial view
Dotted lines show missing tips and oblique lines show broken area

pedicle is smooth. Although the burr is partially broken on the lateral side, it is moderately developed and composed of series of bony nodes. The brow tine is broken, and it might be very small based on the scar of the broken brow tine and close to but relatively high above the burr in munjacks (Fig. 1D). The main beam is thick, developed backward and slightly laterally at first and then curved medially at two thirds of its length. It is flattened near the base. Its cross sections are roughly semicircular or somewhat triangular near the base and become oval at the distal part. The ornamentation of the antler is formed by well-developed longitudinal grooves and crests on the surface of the antler crown.

Table 1 Measurements of antler of *Muntiacus bohlini* from Xinyaozi Ravine and comparison (mm)

Taxon	*M. bohlini*			*M. lacustris*		*M. zhaotongensis*	*M. leilaoensis*
Locality	Shuichongkou	Xiashagou[1)]	Loc. 18[2)]	Yushe[3)]	Juyuandong[4)]	Zhaotong[5)]	Leilao[6)]
Max diameter of distal pedicle	18.9	18.5	12–17.1	16–17	15	16.44–20.10	18.56–18.82
Min diameter of distal pedicle	13.7	13	10–14.5		13.5	14.02–16.94	16.40–15.68
Thickness of burr	4.4	4.9*	4.3			4.56–6.32	5.96–7.22
Max diameter of burr	27.1		21.4	22–32	25?	25.52–33.03	38.78–39.46
Min diameter of burr	21.9		18.7			23.23–29.62	33.12–37.24
Length of antler base	17.5	14.7*	16	16–31		7.38–18.48	12.24–22.32
Angle of bifurcation (°)	50	40	40	50–65		35–40	40
Max diameter of proximal antler base	21.2	24	20–26	17–24	19	16.54–24.36	23.38–30.12
Min diameter of proximal antler base	18.3	23	16–23	14–23	15.6	11.79–16.53	21.22–22.16
Length of the main beam	>76.1	108	72–80	75–92	80	73.23–90.05	125.10
Max diameter of proximal main beam	21.4	22	15–20			16.04–24.42	21.86–23.82
Min diameter of proximal main beam	12.4	14	10.5–14			11.68–16.72	14.58–14.92
Max diameter of proximal brow tine	17.2		9.6	14–26		7.26–9.47	9.74
Min diameter of proximal brow tine	11.3	9.5*	8.4	12–18		4.59–5.89	8.68

Notes: 1) Teilhard de Chardin and Piveteau, 1930; 2) Teilhard de Chardin, 1940; 3) Teilhard de Chardin and Trassaert, 1937; 4) Han, 1987; 5) Dong et al., 2014; 6) Dong et al., 2004; * measured on figure.

The preserved right maxillary fragment (V 26267.2) is composed mainly of three molars (Fig. 2A). The M1, M2 and M3 are all composed of four main cusps; their length and width are close to each other. Accessory elements such as neocrista, entostyle and spur are developed; entocingulum is visible although undeveloped. Measurements of the upper cheek teeth are listed in Table 2.

The p2 is present on V 26267.3 only and simply composed of a main cusp and some minor cusps (Fig. 2B). Its trigonid basin, entoflexid and talonid basin are present and opened lingually. The p3 is present on V 26267.4 and V 26267.5 and composed of two main cusps and some minor cusps (Fig. 2C–D). Paraflexid, trigonid basin, entoflexid and talonid basin are all present and opened lingually, and the hypoflexid is also present. The p4 is also present on V 26267.4 and V 26267.5 and similar to p3, but evidently larger, and metaconid extends mesiodistally (Fig. 2C–D). The dp4 (14.16 mm×7.45 mm×5.7 mm) is present on V 26267.5 and composed of three lobes with a buccal basal pillar between every two lobes (Fig. 2D).

The m1 and m2 are present on all three mandibular fragments and they are all composed of four selenodont main cusps, the *Palaeomeryx* fold is evidently absent, precingulum is present but undeveloped, while ectostylid is developed (Fig. 2B–D). The m3 is present only on

V 26267.4 and composed of three lobes, the anterior two lobes resemble those of m1 and m2, but the third lobe is composed of a developed hypoconulid and a small entoconulid (Fig. 2C).

The measurements of lower cheek teeth are listed in Table 3.

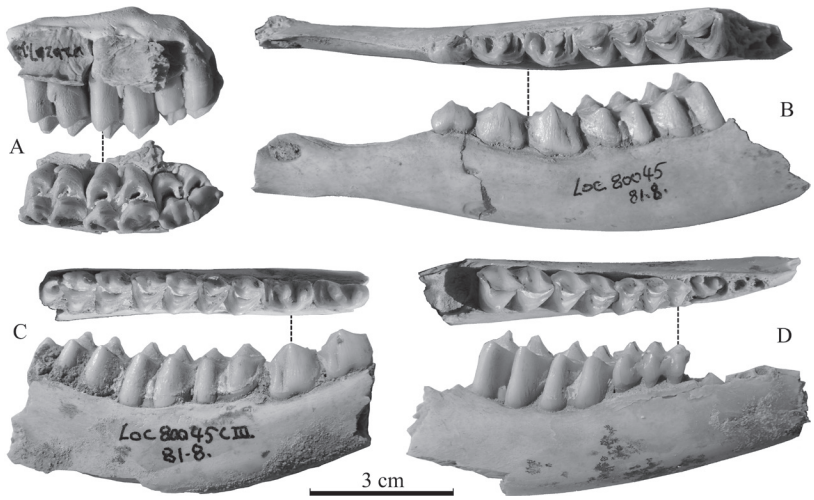

Fig. 2 Cheek teeth of *Muntiacus bohlini* from Xinyaozi Ravine
A. a right maxillary fragment with M1–3 (IVPP V 26267.2), lingual and occlusal views;
B. a left mandibular fragment with p2–m2 (V 26267.3), occlusal and buccal views;
C. a right mandibular fragment with p3–m3 (V 26267.4), occlusal and buccal views;
D. a right mandibular fragment with dp4–m2 (V 26267.5), occlusal and buccal views

Table 2 Measurements of the upper cheek teeth of *Muntiacus bohlini* from Xinyaozi Ravine and comparison (mm)

	M. bohlini		*M. lacustris*	*Muntiacus* sp.	*M. zhaotongensis*
	V 26267.2	RV 4002	Sanhe[1)]	OV 949	Zhaotong[2)]
M1 L	14.18	11.22–12.16	10.5–10.7	10.26–10.86	9.88–10.61
M1 W	13.54	11.02–11.28	13.8–14.1	11.94–11.96	11.35–12.19
M1 H	11.09	5.96–8	4.1–4.2	3.58–3.68	7.81–8.22
M2 L	14.89	11.98–12.44	12.9–13.4	11.96–12.02	10.33–11.13
M2 W	14.88	12.38–13.18	14.6–15.3	13.08–13.18	12.19–13.62
M2 H	13.15	10.36–10.42	8.2–9.2	3.72–4.84	8.75–9.91
M3 L	14.91	12.64–12.76	11.9–13.9	12.54–12.64	9.9–10.51
M3 W	12.81	11.82–12	12.8–13.9	13.06–13.5	11.67–12.88
M3 H	13.01	9.32–11.64	7.7–10.3	4.34–4.88	8.6–8.99
M1–3 L	41.47	36.18–36.2		33.82–34.28	29.88

Notes: 1) Dong et al., 2011; 2) Dong et al., 2014.

Comparison and determination The antler (V 26267.1) is small, its missing brow tine is obviously tiny, its main beam is also small and inclines medially at distal part. It is therefore similar to that from Xiashagou previously identified as *Muntiacus* cf. *sinensis* (Teilhard de Chardin and Piveteau, 1930) and later revised as *M. bohlini* (Teilhard de Chardin, 1940). Its morphology falls well in the variation range of those of *M. bohlini* from Loc. 18 near Beijing (=Peking) (Teilhard de Chardin, 1940). It is also metrically similar to that from Xiashagou and those from Loc. 18 (Table 1). The antler (V 26267.1) is also morphologically close to those of

Table 3 Measurements of the lower cheek teeth of *Muntiacus bohlini* from Xinyaozi Ravine and comparison (mm)

	M. bohlini					*M. lacustris*		*Muntiacus* sp.
	V 26267.3	V 26267.4	V 26267.5	Xiashagou[1)]	Loc. 18[2)]	Sanhe[3)]	Juyuandong[4)]	Longgudong[5)]
p2 L	8.31			8.5*	7*	8.7		7.7
p2 W	4.91					4.6		4.0
p2 H	6.08					8.2		
p3 L	9.07	10.09		9.7*	8.5*			9.2–9.8
p3 W	6.21	6.44						5.2–5.7
p3 H	8.37	8.44						
p4 L	9.68	10.43		9.7*	9.9*	9.5	9.7	10.4
p4 W	7.21	7.32		5.8*		6.9	6.8	6.0
p4 H	9.68	9.75				4.3		
m1 L	13.82	13.84	13.14	13*	12.7*	12.4	11.0	10.1–11.5
m1 W	9.02	9.09	8.05			8.0	7.1	6.9–7.9
m1 H	8.04	7.98	10.2			7.1		
m2 L	14.00	14.30	14.48	15.4*	14.2*	13.0–13.2	11.5	11.0–13.2
m2 W	9.69	9.61	9.49			7.9–8.7	7.6	7.7–8.2
m2 H	10.01	10.34	10.77			9.8–11.8		
m3 L		19.97		19.5*	18.3*	17.3	13.6–17.2	14.2–17.5
m3 W		9.73				9.1	6.8-8.6	7.2–8.5
m3 H		9.23				9.7		
p2–4 L	27.9			27	24–26			
m1–3 L		47.72		46*	38–40			

Notes: 1) Teilhard de Chardin and Piveteau, 1930; 2) Teilhard de Chardin, 1940: 3) Dong et al., 2011; 4) Han, 1987; 5) Chen, 2004; * measured on figures.

M. lacustris from Yushe Basin (Teilhard de Chardin and Trassaert, 1937) and from Juyuandong (Han, 1987). For example, the brow tine is tiny, the main beam is small and curves medially, and the dimensions are close to each other. But its bifurcation position is evidently higher. It differs from those of *M. leilaoensis* (Dong et al., 2004) and *M. zhaotongensis* (Dong et al., 2014) by its smaller burr and simpler curvature of the main beam. It differs from that of *M. hengduanshanensis* from Yunnan (Zong et al., 1996) by thinner and much longer main beam.

The upper dentition (V 26267.2) is generally close to those of *M. bohlini* (RV 4002) from Loc. 18 near Beijing (Teilhard de Chardin, 1940), e.g. presence of spur and entostyle. But its dimensions are slightly larger than those from Loc. 18. Compared with *M. lacustris* from Sanhe in Guangxi (Dong et al., 2011), V 26267.2 is evidently larger (Table 2), and the accessory elements such as neocrista and spur are obvious in V 26267.2 but weak in Sanhe specimens. V 26267.2 is metrically larger than extant *Muntiacus* sp. (OV 949) and the Late Miocene muntjaks from Zhaotong (Table 2). The lower dentitions, represented by two adult and a young mandibular fragments (V 26267.3–5), are close to that of *M. bohlini* from Xiashagou (Teilhard de Chardin and Piveteau, 1930) and Loc. 18 near Beijing (Teilhard de Chardin, 1940) both morphologically and metrically (Table 3). For example, in the p3 and p4, the metaconid is rounded and not fused with paraconid; the paraflexid, trigonid basin, entoflexid, talonid basin and hypoflexid are all present and open in specimens from Taijiaping, Xiashagou and Loc. 18. And for molars, the precingulum is present but undeveloped while ectostylid is developed in specimens from Taijiaping, Xiashagou and Loc. 18. Compared with

M. lacustris from Juyuandong and Sanhe in Guangxi and *Muntiacus* sp. from Longgudong in Hubei, Taijiaping lower dentitions are obviously larger (Table 3).

Both described antler and dentitions are generally in accordance with the diagnosis of *M. bohlini* and evidently different from other muntjaks and can be included into this taxon.

Muntiacus is placed in Muntiacinae under Cervidae based on morphology (e.g. Vislobokova, 1990; Wang, 2003; Azanza et al., 2013; Dong et al., 2018) while Gilbert et al. (2006) suggested to replace the genus into Cervinae based on their analyses of two mitochondrial protein-coding genes and two nuclear introns. But the replacement is not yet widely accepted and we follow the classical classification in the present work.

Pliocervinae Khomenko, 1913

***Cervavitus* Khomenko, 1913**

***Cervavitus* cf. *C. huadeensis* Qiu, 1979**

(Figs. 3–4; Tables 4–6)

Material A right antler fragment with two broken tines (IVPP V 26268.1); a right maxillary fragment with DP4–M2 (V 26268.2) and a right maxillary fragment with DP2–4 (V 26268.3); a right mandibular fragment with dp2–m2 (V 26268.4), a right mandibular fragment with dp3–m3 (V 26268.5) and a right mandibular fragment with dp3–m1 (V 26268.6), all from Taijiaping, Tianzhen, Shanxi.

Description The specimen V 26268.1 is a right antler fragment with two broken tines (Fig. 3A–B). The pedicle emerges from the frontal just above the orbit and inclines backwards (Fig. 3B). The pedicle is thinner than antler base and with moderate length (Table 4). The cross

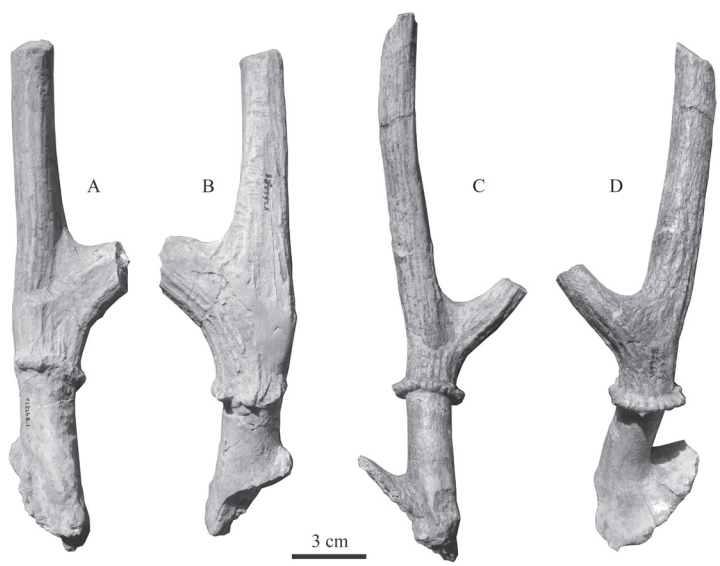

Fig. 3 Comparison of antler of *Cervavitus* cf. *C. huadeensis* from Xinyaozi Ravine with that of *C. shanxius* from Yushe

A, B. right antler of *Cervavitus* cf. *C. huadeensis* (IVPP V 26268.1) from Taijiaping in medial (A) and ventral-lateral (B) views; C, D. the antler of *C. shansius* (V 9378) from Hounao of Yushe in medial (C) and lateral (D) views

Table 4 Measurements of antler of *Cervavitus* cf. *C. huadeensis* from Xinyaozi Ravine and comparison (mm)

Taxon	*C.* cf. *C. huadeensis*	*C. shanxius*		Taxon	*C.* cf. *C. huadeensis*	*C. shanxius*
Locality	Taijiaping	Yushe	Tuchengzi[1)]	Locality	Taijiaping	Yushe
APD pedicle	28.9	21.7	27.8	Bifurcation angle (°)	70	60
TD pedicle	27.6	20.7	26.6	APD stem2	26.7	20.0
L pedicle	36.3	36.5	45.5	TD stem2	24.8	19.46
APD burr	35.8	35.7	37.8	L stem2	>105	>140
TD burr	37.2	33.1	36.1	C stem2	83.9	67
H burr	7.6	7.1	7.6	APD tine1	31.1	16.6
APD stem1	40.2	31	26.2	TD tine1	18.7	13.9
TD stem1	29.1	21	22.9	C tine1	82.5	53
L stem1	71.3	36		L total(burr-tip)	>171	>180
C stem1	113.2	77				

Notes: 1) Dong et al., 2018; APD. anterior-posterior diameter; C. circumference; H. height; L. length; TD. transversal diameter.

sections of the pedicle are oval and the surface of the pedicle is smooth. The burr is not very developed based on the preserved part and is composed of a series of bony nodes. The brow tine is set a short distance above the burr. The main beam is straight as a continuation from the antler base in medial view, but curves smoothly upwards from the antler base in lateral view. The surface of the antler is ornamented with longitudinal crests and furrows.

The DP2 appears as an elongated triangle and the DP3 appears also as a triangle but wider in occlusal view. Both DP2 and DP3 are composed of four selenodont main cusps. Their precingulum is very developed, entocingulum is moderately developed but entostyle (lingual basal pillar) is absent. The DP4 is molarized and composed of four selenodont main cusps (Fig. 4A–B). Its precingulum and entocingulum are moderately developed, and the entostyle and spur are developed. The M1 and M2 are all composed of four main cusps; their length and width are close to each other. The neocrista and entocingulum are visible but not developed, while mesostyle is well developed, entostyle and spur are developed. Measurements of the upper cheek teeth are listed in Table 5.

Table 5 Measurements of upper cheek teeth of *Cervavitus* cf. *C. huadeensis* from Xinyaozi Ravine and comparison (mm)

	C. cf. *C. huadeensis*		*C. fenqii*			*C. shanxius*	
	V 26268.2	V 26268.3	Juyuandong[1)]	Longgudong[2)]	Renzidong[3)]	Tuchengzi[4)]	Hounao[5)]
DP2 L		16.17					11.05–11.80
DP2 W		11.96					7.75–8.05
DP3 L		18.50				12.3–14.7	11.60–14.05
DP3 W		13.75				12.1–15.4	7.55–12.10
DP4 L	17.72	16.68				6.18–13.34	8.10–14.40
DP4 W	16.42	15.62				5.72–13.48	10.15–13.80
M1 L	17.99		14.8–17.0	12.4–19.0	16.81	14.22–17.5	11.25–16.10
M1 W	20.18		17.5–19.6	14.4–20.4	16.55	14.38–17.8	13.40–16.70
M1 H	17.66				13.66	5.54–13.8	4.10–12.90
M2 L	20.51		16.8–20.4	16.8–23.1	18.55	16.4–18.9	13.00–17.50
M2 W	19.13		16.0–20.2	17.4–22.4	18.54	17.5–20.8	15.30–18.50
M2 H	19.83				15.93	7.9–14.5	3.10–13.50
DP2–4 L							33.20–39.30

Notes: 1) Han, 1987; 2) Chen, 2004; 3) Dong et al., 2009; 4) Dong et al., 2018; 5) Dong and Hu, 1994.

The dp2 (Fig. 4C) is dominated by a main selenodont cusp (protoconid). Its crown is little worn and very low when compared with the permanent teeth. The dp3 is dominated by two main cusps (protoconid and hypoconid). Its trigonid basin is widely open but talonid basin is very narrow. The dp4 is molarized and composed of three lobes with developed buccal basal pillars. The m1 and m2 are composed of four selenodont main cusps with evident precingulid and developed ectostylid. The m3 is composed of three lobes. Its anterior two lobes resemble m1 and m2, and the third lobe is small (Fig. 4D). Measurements of the lower cheek teeth are listed in Table 6.

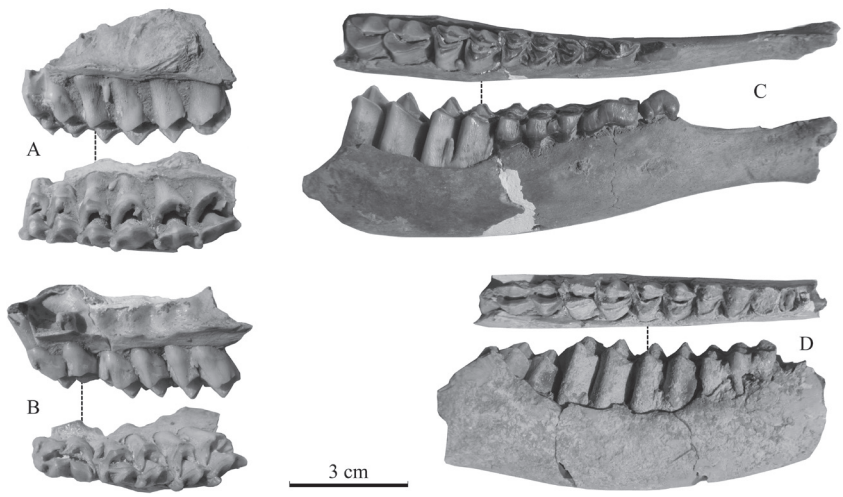

Fig. 4 Cheek teeth of *Cervavitus* cf. *C. huadeensis* from Xinyaozi Ravine
A, B. right maxillary fragments in lingual and occlusal views: A. IVPP V 26268.2, with DP4–M2, B. V 26268.3, with DP2–4; C, D. right mandibular fragments in occlusal and buccal views: C. V 26268.4, with dp2–m2, D. V 26268.5, with dp3–m3

Comparison and determination The described antler (IVPP V 26268.1) is evidently larger than that of *M. bohlini* from Shuichongkou, but it obviously smaller than the antlers of the other cervids from Xinyaozi Ravine. It is morphologically close to that (V 9378, Fig. 3C–D) of *Cervavitus shanxius* from Hounao in Yushe Basin (Dong and Hu, 1994) and that from Tuchengzi (Dong et al., 2018). For example, the pedicle is moderately long and inclines backwards, the brow tine does not emerge from the burr but from the base a short distance above the burr, the first bifurcation angle is moderate. However, Hounao specimen is evidently thinner than Taijiaping one (Fig. 3; Table 4). Compared with *C. huadeensis* from Tuchengzi (Qiu, 1979; Dong et al., 2018), Taijiaping specimen is similar to Tuchengzi specimen V 5634.3 (Qiu, 1979), e.g. the pedicle is not long, the antler base or stem 1 is neither long, the main beam is straight in medial view. But the brow tine is set quite high above the burr in other specimens of *C. huadeensis* (Qiu, 1979) and different from that of Taijiaping. Taijiaping antler differs from those of *C. fenqii* from Juyuandong (Han, 1987), Longgudong (Chen, 2004) and Renzidong (Dong et al., 2009) by larger dimensions. It differs from those of *C. ultimus* (Lin et al., 1978) by its larger angle of the first bifurcation.

The described upper cheek teeth are characterized by the presence of neocrista, spur and entostyle. The neocrista is present in *C. shanxius* from Hounao and Tuchengzi but more developed than in Taijiaping specimens. The spur and entostyle are similarly developed in Taijiaping as well as in Hounao and Tuchengzi specimens. The upper dentition of *C. huadeensis* is not yet available from Tuchengzi specimens. Compared with *C. fenqii* from Juyuandong (Han, 1987), Longgudong (Chen, 2004) and Renzidong (Dong et al., 2009), Taijiaping specimens also have developed entostyle, but have evident neocrista and developed spur which are absent in Juyuandong and Longgudong specimens. In addition, Taijiaping specimens are slightly larger (Table 5). The lower cheek teeth from Taijiaping are generally similar to those of *C. huadeensis* from Tuchengzi (Dong et al., 2018) both morphologically and metrically (Table 6). Taijiaping specimens are evidently larger than those of *C. fenqii* from Juyuandong, Longgudong and Renzidong, as well as those of *C. shanxius* from Hounao and Tuchengzi (Table 6).

Table 6 Measurements of the lower cheek teeth of *Cervavitus* cf. *C. huadeensis* from Xinyaozi Ravine and comparison (mm)

	C. cf. *C. huadeensis*			*C. huadeensis*	*C. fenqii*			*C. shanxius*	
	V 26268.4	V 26268.5	V 26268.6	Tuchengzi[1)]	Juyuandong[2)]	Longgudong[3)]	Renzidong[4)]	Tuchengzi[1)]	Hounao[5)]
dp2 L	10.07			9.4				8.26–9.72	7.50–10.35
dp2 W	5.08			5.1				3.96–5.18	3.75–5.45
dp3 L	15.20		14.88	14.3				11.58–13.42	10.35–13.70
dp3 W	7.10		7.20	7.52				5.72–6.42	4.40–6.70
dp4 L	21.98	20.20	22.22	21.98				17.36–19.6	6.70–8.80
dp4 W	10.60	9.92	9.50	10.0				8.1–8.52	6.70–8.80
m1 L	17.15	18.03	19.17	19.42	12.9–15.7	14.4–15.8	14.58–17.38	12.56–16.7	11.80–15.70
m1 W	02.30	11.44	10.50	11.2	10.5–12.0	9.5–11.0	11.09–11.34	9.38–10.8	8.50–11.00
m1 H	14.07	14.61	13.50	15.3			6.48–11.81	3.4–11.4	4.30–11.20
m2 L	21.54	20.19		23.78	16.8–19.5	16.8–18.3	18.27–19.21	15.1–18.7	13.90–17.20
m2 W	12.47	12.25		13.6	12.2–13.2	11.3–12.2	10.80–12.42	10.78–12.36	9.80–12.00
m2 H	21.44	19.06		16.7			10.92	4.9–15.0	4.90–13.00
m3 L		24.47			22.6–23.0	22.4–26.7	24.60–27.09	20.3–22.9	17.70–24.20
m3 W		11.08			11.6–14.6	10.5–14.1	12.07–12.72	11.12–11.78	9.25–11.60
m3 H		17.30					13.62–20.90	5.68–13.0	5.70–13.00
dp2–4 L	44.80			45.34				36.28–40.7	33.70–42.10
m1–3 L		67.76						48.4–56.1	44.90–54.60

Notes: 1) Han, 1987; 2) Chen, 2004; 3) Dong et al., 2009; 4) Dong et al., 2018; 5) Dong and Hu, 1994.

The comparison between Taijiaping specimens and those of *Cervavitus* from other localities indicates that Taijiaping specimens are closer to those of *C. huadeensis* from Tuchengzi than those of *C. fenqii* and *C. shanxius*. But there are still some differences between Taijiaping specimens and those of *C. huadeensis*, e.g., the ornamentation of antler in Tuchengzi antlers are more developed than in Taijiaping specimens, ectostylid is less developed in Tuchengzi lower molars. In addition, *C. huadeensis* are previously uncovered from the Neogene deposits rather than in the Pleistocene ones, and the material from Taijiaping is limited to a broken antler and some fragmental jaws. We place them temporarily as a conformis species of *C. huadeensis*.

Cervinae Goldfuss, 1820

Axis Smith, 1827

Axis shansius Teilhard de Chardin & Trassaert, 1937

(Figs. 5–6; Tables 7–9)

Axis shansius Teilhard de Chardin and Trassaert, 1937, p. 44–50

Axis cf. *shansius* Chi, 1975, p. 173

Axis shansius Chia and Wang, 1978, p. 21–23

Axis shansius Dong and Fang, 2004, p. 299–302

Axis shansius Dong, 2006, p. 335–338

Axis shansius Bai et al., 2017, p. 821–823

Material A large part of a left antler with partial frontal (IVPP V 26264.1); a left maxillary fragment with DP2–M1 (V 26264.2), a left maxillary fragment with a broken DP3 and complete DP4 and M1 (V 26264.3), a left maxillary fragment with DP3–4 (V 26264.4); a right mandibular fragment with p2–m3 (V 26264.5), a left mandibular fragment with a broken p2 and completed p3–m3 (V 26264.6), a left mandibular fragment with dp2–m1 (V 26264.7). All specimens are from Taijiaping, Tianzhen, Shanxi.

Description The specimen V 26264.1 is a large part of a left antler with partial frontal (Fig. 5; see Table 7 for measurements). The pedicle is relatively short, and its cross sections are oval. The burr is composed of a series of developed bony nodules. The antler base, or stem 1, is relatively short. The distance between the first bifurcation and the burr is similar to that between the frontal and burr. The brow tine is long and curved in the middle. The main beam is very long and lyrately curved. The first bifurcation angle is very large, but the second one is relatively small. The second and third tines are broken near their base. The surface of the antler is ornamented with developed longitudinal crests and furrows.

Fig. 5 Lateral view (left) and medial view (right) of the left antler of *Axis shansius* (IVPP V 26264.1) from Taijiaping

Table 7 Measurements of antler of *Axis shansius* from Taijiaping and comparison (mm)

	V 26264.1	Yushe Larger[1)]	Yushe Smaller[1)]	Xihoudu[2)]	Jinyuandong[3)]
APD pedicle	38.1				
TD pedicle	42.1	32–43	26	55	
L pedicle	53.3	37–50	40	44	
APD burr	69.6	50–58	37–48	63–78	
TD burr	62.5				
H burr	10.4				
APD base	60.3	35–45	26–35	55–73	
TD base	55.4				
APD stem1	67.1				
TD stem1	49.9				
L stem1	81.1	66–130	67–74	62–94	
C stem1	197.2				
APD stem2	45.3	28–42	22–25	41–51	42.31
TD stem2	42.5				39.80
L stem2	506.2	430–507	255–315	360–470	245
C stem2	149.6				
APD tine1	40.7				
TD tine1	36.1				
L tine1	250.1	162–280	111–127	196–226	
C tine1	137.4				
APD tine2	28.3	14–34	12–15		36.5
TD tine2	28.2				29.1
APD tine3	28.7	20–34	14–25		36.6
TD tine3	32.9				28.3
L total (burr-tip)	>607	724–985	461–490		
Angle 1st bifurcation	105°	63–117°	84–110°	85–140°	
Angle 2nd bifurcation	60°				75°

Notes: 1) Teilhard de Chardin and Trassaert, 1937; 2) Chia and Wang, 1978; 3) Bai et al., 2017. For abbreviations see Table 4.

The DP2 appears as an elongated triangle (Fig. 6A) and the DP3 (Fig. 6A, C) also but wider in occlusal view. Both DP2 and DP3 are composed of four selenodont main cusps. Their precingulum is very weak, entocingulum is moderately developed and entostyle (lingual basal pillar) is present. The DP4 is molarized and composed of four selenodont main cusps (Fig. 6A–C). Its precingulum is absent, and its entocingulum is moderately developed, while the entostyle and spur are developed. The M1 are all composed of four main cusps; their length and width are close to each other (Fig. 6A–B). The precingulum, neocrista and entocingulum are visible but very weak, while mesostyle, entostyle and spur are developed. The M2 and M3 are not available but might be similar to the M1. Measurements of the upper cheek teeth are listed in Table 8.

The dp2 (Fig. 6F) is dominated by a main selenodont cusp (protoconid). The dp3 (Fig. 6F) is dominated by two main cusps (protoconid and hypoconid). Its trigonid basin is widely open but talonid basin is very narrow. The dp4 (Fig. 6F) is molarized and composed of three lobes with developed buccal basal pillars. The p2 (Fig. 6D) is dominated by a main selenodont cusp (protoconid), its trigonid and talonid basins are weak but entoflexid is very developed. The p3 (Fig. 6D–E) is also dominated by protoconid. The trigonid basin is well developed

and widely open. The entoflexid and talonid basin are very narrow. The p4 (Fig. 6D–E) is dominated by protoconid and metaconid. The metaconid does not extend forwards but backwards. The trigonid basin is moderately developed and open. The entoflexid and talonid basin are narrow but still open. The m1 (Fig. 6D–F) and m2 (Fig. 6D–E) are composed of four selenodont main cusps. The m3 (Fig. 6D–E) is composed of three lobes. Its anterior two lobes resemble the m1 and m2, and the third lobe is small. The *Palaeomeryx* fold and goat fold are

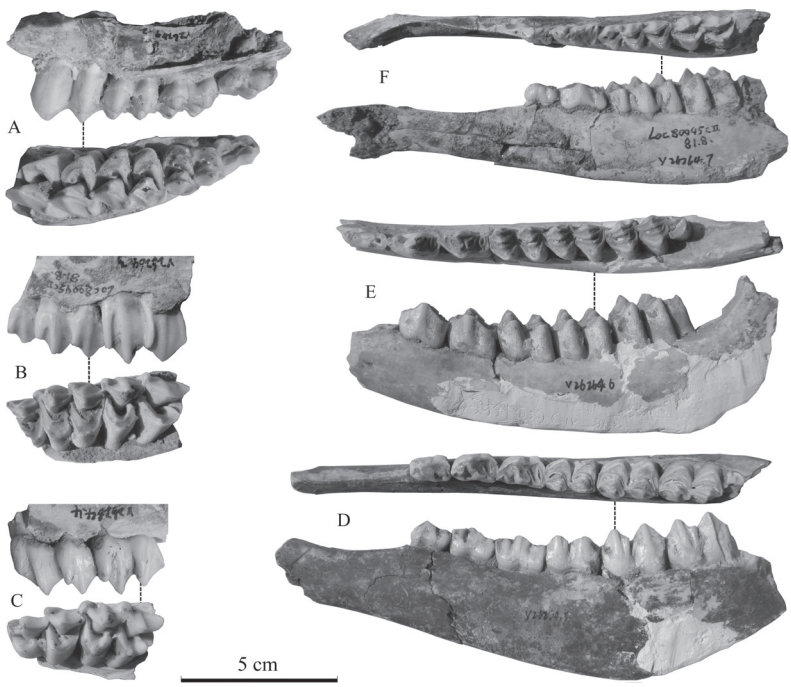

Fig. 6 Cheek teeth of *Axis shansius* from Taijiaping

A. IVPP V 26264.2, a left maxillary fragment with DP2–M1 in lingual and occlusal views; B. V 26264.3, a left maxillary fragment with a broken DP3 and complete DP4 and M1 in buccal and occlusal views; C. V 26264.4, a left maxillary fragment with DP3–4 in buccal and occlusal views; D. V 26264.5, a right mandibular fragment with p2–m3 in occlusal and lingual views; E. V 26264.6, a left mandibular fragment with a broken p2 and completed p3–m3 in occlusal and buccal views; F. V 26264.7, a left mandibular fragment with dp2–m1 in occlusal and buccal views

Table 8 Measurements of upper cheek teeth of *Axis shansius* from Taijiaping and comparison (mm)

	V 26264.2	V 26264.3	V 26264.4	Yushe[1)]	Tuozidong[2)]	Dajushan[3)]
DP2 L	15.28					
DP2 W	11.91					
DP3 L	18.56		20.15			
DP3 W	14.27	15.5	16.28			
DP4 L	18.90	19.41	20.43			
DP4 W	17.16	19.13	18.49			
M1 L	22.83	22.92		18	19.74–21.99	18.20–19.22
M1 W	21.25	22.79		17–19	19.71–23.07	16.90–19.20
M1 H	21.09	19.45			8.10–14.75	15.34–16.00
DP2–4 L	52.5					

Notes: 1) Teilhard de Chardin and Trassaert, 1937; 2) Dong, 2006; 3) Dong and Fang, 2004.

absent in all molars, but precingulid is present and weak on the m1 and absent on the m2 and m3. The ectostylid (buccal basal pillar) is developed on the m1, evident on the m2 and fully-grown on the m3. Measurements of the lower cheek teeth are listed in Table 9.

Table 9 Measurements of lower cheek teeth of *Axis shansius* from Taijiaping and comparison (mm)

	V 26264.5	V 26264.6	V 26264.7	Yushe[1)]	Tuozidong[2)]	Dajushan[3)]
dp2 L			9.78			
dp2 W			5.11			
dp3 L			14.52			
dp3 W			7.02			
dp4 L			21.90			
dp4 W			9.18			
p2 L	13.17	13.9			12.79–15.59	11.98
p2 W	8.68	>6.0			6.92–7.77	6.96
p2 H	9.58				7.00–10.31	10.20
p3 L	14.94	15.98		15.0	16.00–20.95	17.30
p3 W	9.81	8.30		9.2	8.45–11.78	8.70
p3 H	11.13	12.73		9.3	8.05–14.31	12.10
p4 L	16.58	16.56		16.8	16.48–22.38	16.90
p4 W	11.09	9.32		9.5	10.12–14.09	9.50
p4 H	12.22	12.35		9.4	7.96–15.71	15.30
m1 L	16.94	18.23	18.24		18.80–23.82	16.70–19.70
m1 W	12.56	12.13	10.64		11.49–15.68	8.70–11.30
m1 H	10.50	12.61	12.71		3.82–15.69	12.40–13.80
m2 L	20.47	19.77		20.0	19.13–26.13	18.32–21.30
m2 W	14.31	12.20		14.0	13.53–17.05	11.60–14.30
m2 H	15.53	13.32		10.0	5.51–15.80	10.60–16.80
m3 L	27.19	26.57		28.5	26.09–32.70	24.76–28.36
m3 W	14.17	12.85		14.1	13.14–15.70	8.60–11.38
m3 H	15.01	15.63		13.8		11.60–16.00
dp2–4 L			46.30			47.50
p2–4 L	44.67	46.8			45.41–52.31	
m1–3 L	66.33	62.61		65	70.89–76.53	67.00
p2–m3 L	112.33	113.6		110	121.52–126.28	

Notes: 1) Teilhard de Chardin and Trassaert, 1937; 2) Dong, 2006; 3) Dong and Fang, 2004.

Comparison and determination The described antler has unbranching brow tine and bifurcated posterior beam that distinguishes it from *Elaphurus* although its size is similar to that of the latter. It differs from stratigraphically associated *Cervavitus* cf. *C. huadeensis* by its long and lyrated main beam. It fits well the diagnosis of *Axis shansius* (Teilhard de Chardin and Trassaert, 1937) by its lyrated main beam with three tines and widely opened first fork, as well as its very long first tine (brow tine). Compared with *A. shansius* from Yushe, Taijiaping antler is very close to the antler of THP 12387 (=No. 12.387) (Teilhard de Chardin and Trassaert, 1937), although its main beam is less curved than that of the type. The dimensions of Taijiaping antler falls well in variation range of antlers of *A. shansius* from Yushe (Table 7). Both upper and lower dentitions of Taijiaping specimens are also metrically similar to those of *A. shansius* from Yushe (Tables 8–9). Taijiaping antler is also close to that of *A. shansius* from Xihoudu (Chia and Wang, 1978), e.g. three-tined antler, and lyrated main beam. But the first bifurcation of Xihoudu specimens is closer to the burr, and the first bifurcation angle is larger.

Taijiaping antler is similar to that of *A. shansius* from Tuozidong (Dong and Fang, 2004) and Jinyuandong (Bai et al., 2017), e.g. the curvature of the main beam and the form of the second bifurcation. Both upper and lower dentitions of Taijiaping specimens share the same morphological traits with those from Tuozidong and Dajushan (Dong, 2006), e.g. the accessary elements such as precingulum, entostyle, spur etc. are present. Their dimensions are also close to each other (Tables 8–9).

Compared with other species of *Axis*, Taijiaping specimens are much larger than those of *A. speciosus* from Ertemte in Nei Mongol (Schlosser, 1924). For example, the main beam of Taijiaping specimen is twice longer, the burr is twice thicker, the dentitions are nearly one and half larger. Taijiaping antler is moderately longer and thicker than that of *A. rugosus* from Tongshan at Yuanqu in Shanxi (Chow, 1954). In addition, the brow tine is set very close to the burr (as in extant *A. axis*), the furrow ornamentation is very developed in Tongshan antler. Taijiaping antler is moderately longer but slightly thinner than that of *A. lingjingensis* from Lingjing Man site in Henan (Dong and Li, 2008, Bai et al., 2017), and its first bifurcation angle is larger than that in Lingjing specimens. Taijiaping specimens are therefore morphologically and metrically closest to *A. shansius* and clearly different from other species of *Axis*.

Nipponicervus Kretzoi, 1941

Nipponicervus elegans (Teilhard de Chardin & Piveteau, 1930)

(Figs. 7–8; Tables 10–12)

Cervus (*Rusa*) *elegans* Teilhard de Chardin and Piveteau, 1930, p. 54–63

Rusa elegans Wei, 1997, p. 196

Material A broken skull with a pair of broken antlers (IVPP V 26265.1), a broken right antler with pedicle and partial frontal (V 26265.2), a broken left antler with pedicle and partial frontal (V 26265.3); specimens V 26265.1–3 are from Taijiaping. A left maxillary fragment with P2–M3 (V 26265.4), a right maxillary fragment with P2–M3 (V 26265.5), a left maxillary fragment with P3–M3 (V 26265.6), a right maxillary fragment with P2–4 (V 26265.7), a right mandibular fragment with p4–m3 (V 26265.8), a left mandibular fragment with p2–m3 (V 26265.9), a left mandibular fragment with p3–m2 (V 26265.10) and a right mandibular fragment with p4–m3 (V 26265.11) from Xinyaozi Ravine, Tianzhen, Shanxi.

Description Although the referred antlers are all broken, the length of broken main beams indicates the antlers bifurcate at least twice and with at least three tines. The specimen V 26265.1 is a broken skull with a pair of broken antlers (Fig. 7A–B). The frontals are flat and wide in anterior view. Two pedicles, relatively short, emerge from lateral-posterior parts of the frontals above the orbits and extend backwards and laterally. The distance between the bases of two pedicles measures 37 mm. The angle between two pedicles is about 60°. The cross sections of the pedicles are oval. The burrs are composed of a series of bony nodules and moderately developed although partially broken. The antler base or stem 1 of the pair is well preserved and moderately long. The first bifurcation angle is 50°–65°. The first tine (brow tine) is relatively long (Table 10) and slightly curves medially. Both left and right first tines are broken near their

tips. Both left and right main beams are also broken. The surface of the antler is ornamented with longitudinal crests and furrows.

The specimen V 26265.2 is a broken right antler with pedicle and partial frontal (Fig. 7C–D). It is very similar to the right antler of the specimen V 26265.1 described above, e.g. relatively short pedicle with oval cross sections, burr formed with a ring of bony nodules, antler base and the first tine moderately long (Table 10). But its main beam continuously curves laterally and posteriorly instead of laterally and upwards. It is also ornamented with longitudinal crests and furrows and with some bony nodules or pearled on medial side.

The specimen V 26265.3 is a broken left antler with pedicle and partial frontal (Fig. 7E–F). It is also very similar to the specimen V 26265.1 (see Table 10 for measurements). But its ornamentation has many bony nodules on medial side in addition to longitudinal crests and furrows.

The P2 is semi-molarized, the lingual main cusps (protocone and metaconule) are separated by entoflexus, but the buccal main cusps (paracone and metacone) are fused end to end (Fig. 8A–B). The neocrista is developed, entocingulum is very weak, but the precingulum, entostyle and spur are absent. The P3 is similar to P2, but with larger dimensions (Fig. 8A–C).

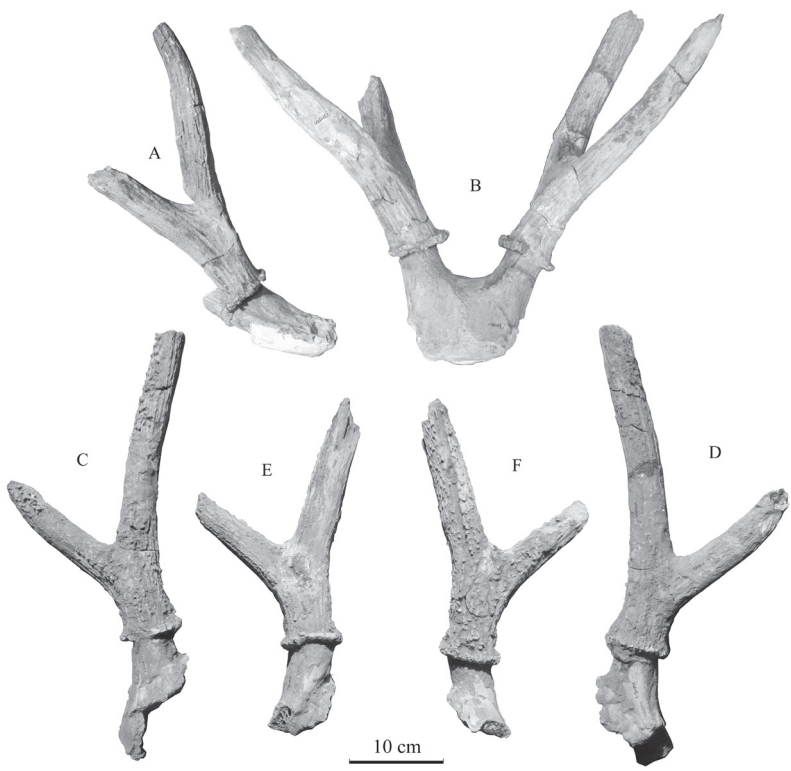

Fig. 7 Antlers of *Nipponicervus elegans* (IVPP V 26265.1–3) from Taijiaping
A, B. IVPP V 26265.1, a broken skull with a pair of broken antlers: A. lateral view of the right antler, B. anterior view; C, D. V 26265.2, a broken right antler with pedicle and partial frontal in medial (C) and lateral (D) views; E, F. V26265.3, a broken left antler with pedicle and partial frontal in lateral (E) and medial (F) views

Table 10 Measurements of antlers of *Nipponicervus elegans* from Taijiaping and comparison (mm)

	V 26265.1L	V 26265.1R	V 26265.2	V 26265.3	Xiashagou[1)]	Yushe[2)]	Longdan[3)]
APD pedicle	34.3	35.9	45.9	40.9	32		48
TD pedicle	40.5	39.7	44.2	43.8			41
L pedicle	39.4	38.3	53.8	39.3	40–42		30
APD burr		58.7	67.7	62.7	50	38	
TD burr	62.3	65.2		63.2			
H burr	6.9	9.6	10.2	9.4			
APD base	45.2	46.1	55.1	50.7			
TD base	46.1	50.6	50.4	50.2			
APD stem1	44.6	53.1	58.3	53.1	55		
TD stem1	41.5	41.8	46.6	41.3			
L stem1	108.9	88.9	92.7	94.2	67–95	115	56
C stem1	145.2	153.2	164.5	166.4	125–192		
APD stem2	33.3	35.7	37.6	40.4	27	34	48
TD stem2	30.6	34.6	35.4	38.3			31
L stem2	>209.2	>111.2	>238.6	>182.3	225	382	517
C stem2	115.9	117.2	122.3	127.6			
APD tine1	32.6	33.8	36.4	34.5			39
TD tine1	29.2	39.6	42.3	29.3			
L tine1	225.3	>160.4	310.9	>111.7	114	117	310
C tine1	98.9	111.5	112.2	109.1			
L total(burr-tip)	>302.1	>199.3	>318.9	>256.9	380		800
Angle 1st bifurcation	65°	50°	65°	65°	60°	45°	80°

Notes: 1) Teilhard de Chardin and Piveteau, 1930; Teilhard de Chardin and Trassaert, 1937; 2) Teilhard de Chardin and Trassaert, 1937; 3) Qiu et al., 2004. For abbreviations see Table 4.

The P4 is one lobed and evidently different from P2 and P3, the anterior and posterior main cusps on both lingual and buccal sides are fused end to end; the precingulum, entocingulum, entostyle and spur are all absent, but neocrista is still present and developed (Fig. 8A–C). The M1 is composed of four main cusps; its length and width are close to each other (Fig. 8A–C). The neocrista is absent, precingulum and entocingulum are visible but not developed, while mesostyle, entostyle and spur are developed. The morphology of M2 is similar to that of M1, but its size is larger than that of M1 and its length is slightly larger than its width; there is a fold on the lingual side of postprotocrista (posterior crest of protocone) equivalent to the *Palaeomeryx* fold of lower molar. It differs from neocrista by its position on the lingual side, instead of buccal side, of postprotocrista. The morphology of M3 is also similar to that of the M1, but its length is evidently larger than its width. Measurements of the upper cheek teeth are listed in Table 11.

The p2 (Fig. 8E) is dominated by a main selenodont cusp (protoconid); the paraflexid is absent, its trigonid basin is developed and widely open, its entoflexid and talonid basins are very narrow, its hypoflexid is very weak. The p3 (Fig. 8E–F) is also dominated by protoconid; its paraflexid is present but very weak, its trigonid basin is well developed and widely open, its entoflexid and talonid basins are relatively narrow, its hypoflexid is moderately developed. The p4 (Fig. 8D–E) is dominated by protoconid and metaconid; its paraflexid is weak and open, its metaconid extends moderately forwards and backwards but leaves trigonid basin and entoflexid open; entoconid inclines backward and nearly closes talonid basin. The m1 (Fig.

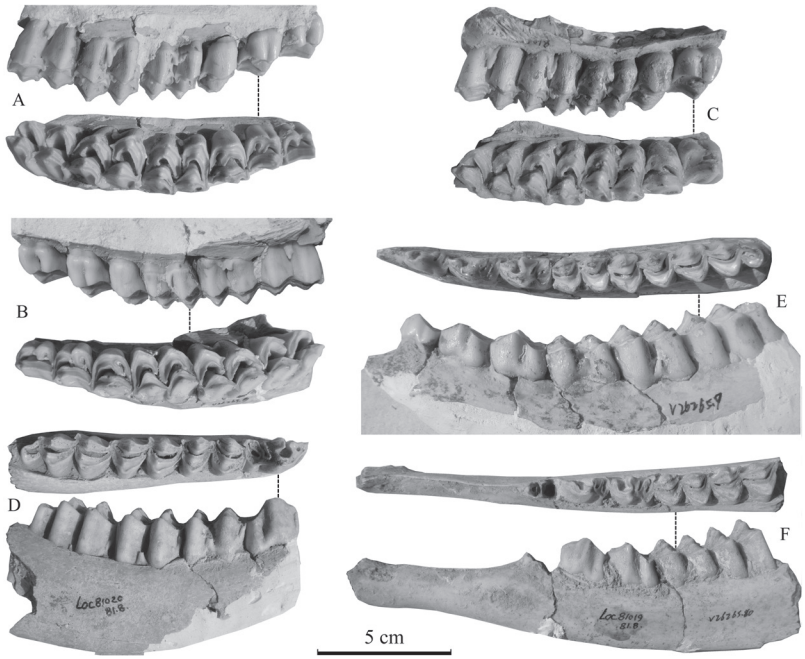

Fig. 8 Cheek teeth of *Nipponicervus elegans* from Xinyaozi Ravine
A. IVPP V 26265.4, a left maxillary fragment with P2–M3 in lingual and occlusal views; B. V 26265.5, a right maxillary fragment with P2–M3 in lingual and occlusal views; C. V 26265.6, a left maxillary fragment with P3–M3 in lingual and occlusal views; D. V 26265.8, a right mandibular fragment with p4–m3 in occlusal and buccal views; E. V 26265.9, a left mandibular fragment with p2–m3 in occlusal and buccal views; F. V 26265.10, a left mandibular fragment with p3–m2 in occlusal and buccal views

Table 11 Measurements of upper cheek teeth of *Nipponicervus elegans* from Xinyaozi Ravine and comparison (mm)

	N. elegans					*N. longdanensis*	*Arvernoceros ardei*
	V 26265.4	V 26265.5	V 26265.6	V 26265.7	Xiashagou[1)]	Longdan[2)]	Etouaires[3)]
P2 L	16.56	17.62		16.42		16.5	14–16
P2W	16.70	16.39		15.30		14	13.5–17.5
P2 H	13.64	14.68		15.96			
P3 L	16.59	17.03	16.31	16.13		19	14–15.5
P3 W	18.85	19.08	18.50	17.82		17.8	15.5–17.5
P3 H	13.74	16.07	15.82	19.15			
P4 L	15.15	15.24	14.16	14.73		17	13.5–15.5
P4 W	19.38	18.68	20.20	19.18		20.2	17–20
P4 H	14.68	14.95	15.04	16.32			
M1 L	22.98	22.61	20.64		28		19–22
M1 W	22.98	22.28	20.91		25		20–23.5
M1 H	15.75	17.53	13.04				
M2 L	24.42	24.62	22.85			26	19–25.5
M2 W	23.26	23.10	23.93			23.5	21.5–26.5
M2 H	20.71	18.86	16.78				
M3 L	24.90	25.38	23.05			27.3	20–24.5
M3 W	21.43	22.45	22.90			25.5	21.5–25.5
M3 H	19.80	19.92	17.64				
P2–4 L	50.60	52.04		49.95	43–55	51	43–46.5
M1–3 L	70.9	71.61	63.39		60–77	72	58.5–68.5
P2–M3	116.97	117.93			103–136	120	97.5–104.5

Notes: 1) Teilhard de Chardin and Piveteau, 1930; 2) Qiu et al., 2004; 3) Heintz, 1970.

8D–F) and m2 (Fig. 8D–F) are composed of four selenodont main cusps; the *Palaeomeryx* fold and goat fold are absent, but precingulid is present and weak, ectostylid (buccal basal pillar) is developed; the dimensions of m2 are evidently larger than those of m1. The m3 (Fig. 8D–E) is composed of three lobes. Its anterior two lobes resemble the m1 and m2, and the third lobe is small. Measurements of the lower cheek teeth are listed in Table 12.

Table 12 Measurements of lower cheek teeth of *Nipponicervus elegans* from Xinyaozi Ravine and comparison (mm)

	N. elegans					*N. longdanensis*	*Arvernoceros ardei*
	V 26265.8	V 26265.9	V 26265.10	V 26265.11	Xiashagou[1)]	Longdan[2)]	Etouaires[3)]
p2 L		14.41	17.52				11.5–15
p2 W		8.04	7.66				6.5–9.5
p2 H		8.96					
p3 L		17.36	18.44				15–20.5
p3 W		10.28	11.48				9–12.5
p3 H		11.72	14.20				
p4 L	21.96	18.96	19.18	19.39	16–22		15–21
p4 W	12.29	11.18	12.35	10.61	10–14		9.5–13.5
p4 H	18.65	12.93	15.94	12.19			
m1 L	23.66	19.63	21.29	20.16		24.41	16.5–24
m1 W	15.94	13.85	14.24	14.67		13.73	12.5–15
m1 H	17.27	12.81	11.62	10.51		26.16	
m2 L	27.64	2.87	25.56	21.34			20.5–25.5
m2 W	18.03	15.52	15.84	16.14			14–16.5
m2 H	18.22	14.21	15.99	16.06			
m3 L	34.40	30.39		29.63			28–35
m3 W	17.75	14.34		16.34			13–15.5
m3 H	19.90	14.56		17.05			
p2–4 L		50.57	51.68		52–56		43–53
m1–3 L	82.37	72.51		71.45	70–89		65–77.5
p2–m3 L		121.85			112–145		108–129.5

Notes: 1) Teilhard de Chardin and Piveteau, 1930; 2) Wang, 2014; 3) Heintz, 1970.

Comparison and determination The type and associated specimens of *Nipponicervus elegans*, previously named as *Cervus* (*Rusa*) *elegans*, were collected from Xiashagou area, i.e. type locality, in Nihewan Basin (Teilhard de Chardin and Piveteau, 1930). Compared with Xiashagou specimens, Xinyaozi specimens are very close to those from type locality. For example, pedicle relatively short, the antler base is moderately long, the first bifurcation angle is moderate, the main beam is nearly straight, the brow tine is relatively long and slightly curves medially; the entoflexus is developed on P2 and P3, entostyle is developed on upper molars; trigonid basin is well open on p3 and p4 and ectostylid is developed on lower molars. The dimensions of antlers and dentitions are also very close (Tables 10–12). In addition, Xinyaozi specimens are geographically and stratigraphically close to Xiashagou specimens and they can be regarded as the same species. Some antlers from Yushe Basin were resigned to *Cervus* (*Rusa*) cf. *elegans* (Teilhard de Chardin and Trassaert, 1937). They were revised as *N. elegans* (Qiu et al., 2004). Xinyaozi specimens are also similar to those from Yushe.

Compared with *N. longdanensis* from Longdan (Qiu et al., 2004), Xinyaozi antlers are similar by relatively long brow tine, nearly straight main beam, but different by longer antler

base, smaller angle of the first bifurcation (Table 10). The Xinyaozi dentitions are also similar to that from Longdan (Tables 11–12).

Nipponicervus elegans from Xinyaozi and Xiashagou are comparable with *Cervus rhenanus* (Heintz, 1970; de Vos et al., 1995) in Europe. However, the antlers of the latter are slenderer and the dentitions are smaller. *N. elegans* from Xinyaozi and Xiashagou are also comparable with *Arvernoceros ardei* from Étouaires in France (Heintz, 1970), especially for dimensions of dentitions (Tables 11–12). Nevertheless, the main beams are much longer and more curved, and the entocingulum of upper cheek teeth is very developed in French specimens.

Cervus (*Elaphus*) Smith, 1827

Cervus (*E.*) *elaphus* Linnaeus, 1758

(Fig. 9; Table 13)

Material An incomplete right antler with pedicle and partial frontal (IVPP V 26266) from Dazhuangkecun (Dazhuangke village), about 3 km southwest of Taijiaping, Tianzhen, Shanxi.

Description The specimen V 26266 is a right adult antler with pedicle and partial frontal (Fig. 9). The pedicle is relatively short and evidently thinner than the antler base; its cross sections are oval. The burr is well developed and preserved. It is composed of a series of bony nodules. The antler base, Stem 1, is very short, with elongated oval cross sections. The brow tine is broken but its base is preserved. Its preserved part indicates that it emerges from the antler base, or stem 1, anteriorly and upwards. It is set very low, almost on the burr. The bez tine is absent, i.e. not developed at all. The trez tine is nearly complete, only its tip part is

Fig. 9 Medial (left) and lateral (right) views of the right antler (IVPP V 26266) of *Cervus elaphus* from Dazhuangke

missing; it is moderately long and curves slightly upwards. Stem 2, the main beam between the first and second bifurcations, or between the bases of brow and trez tines, is relatively long; its cross sections are somewhat triangular near the first bifurcation and become elongated oval towards the second bifurcation. The part about 95 mm above the second bifurcation is missing. The ornamentation is composed of moderate longitudinal furrows and without crests.

Comparison and determination The described antler is evidently different from the other specimens from Xinyaozi by its large size and large angle of the first bifurcation. It is very close to that of red deer, e.g. the brow tine set very low and almost on the burr, the angle between brow tine and the main beam is very large (Table 13), etc. But it has no bez tine as in some European red deer, such as *Cervus elaphus aretinus* from Veneto to Calabria in Italy (Abbazzi, 1995). Compared with *C. canadensis mongoliae* from northern China (Zdansky, 1925), Dazhuangke specimen lacks bez tine and is slightly larger (Table 13), the rest morphological characters are very similar. Compared with *Cervus* cf. *C. canadensis* from Yushu in northeastern China (Xue, 1959), besides the bez tine on the antlers from Yushu, Dazhuangke specimen appears more robust, but the burrs are more developed in Yushu specimens.

Table 13 Measurements of antler of *Cervus elaphus* from Dazhuangke and comparison with that of *C. canadensis mongoliae* (mm)

	V 26266	*C . canadensis mongoliae*[1)]		V 26266	*C . canadensis mongoliae*[1)]
APD pedicle	56.7		APD stem3	49.4	
TD pedicle	54.5		TD stem3	50.5	
L pedicle	37.6		L stem3	>94.4	235
APD burr	90.8	81	C stem3	164.3	
TD burr	65.4		APD tine1	39.1	
H burr	11.1		TD tine1	38.2	
APD base	80.6	74	L tine1	>50	
TD base	66.7		C tine1	237	
APD stem1	85.5	72	APD tine2	42.2	
TD stem1	56.2		TD tine2	36.1	
L stem1	36.2		L tine2	>198.2	
C stem1	238		C tine2	120.9	
APD stem2	53.1		L total(burr-tip)	>403.5	1090
TD stem2	55.1		Angle 1st bifurcation	120°	120°
L stem2	282.5		Angle 2nd bifurcation	80°	87°
C stem2	175.1		Angle 3rd bifurcation		80°

Notes: 1) Zdansky, 1925. For abbreviations see Table 4.

3 Discussion and conclusion

Muntiacus bohlini was established by Teilhard de Chardin (1940) for the specimens from Loc. 18, and he reassigned *Muntiacus* cf. *M. sinensis* from Xiashagou (Teilhard de Chardin and Piveteau, 1930) to this species. The present study on the material from Xinyaozi reconfirmed the presence of the taxon in Nihewan Formation. The extant muntjaks range only in China, southern and southeastern Asia (Nowak and Paradiso, 1983). The earliest

muntjak, *M. noringenensis*, was found at Tuosu Nor in the eastern Qaidam of the Qinghai-Tibetan Plateau from the lower part of the Upper Youshashan Formation (9–11 Ma), the Late Miocene (Dong, 2007). It is a relatively large muntjak and it indicates probably the genus originated in the Qinghai-Tibetan Plateau. The second earliest muntjak, *M. leilaoensis*, was discovered at Leilao hominoid locality, Yuanmou in Yunnan Province (Dong et al., 2004) from lower part of Xiaohe Formation (8.2–7.2 Ma), the Late Miocene (Qi et al., 2006). It is much smaller than *M. noringenensis* and very close to the extant muntjaks. *M. zhaotongensis* was uncovered at Shuitangba hominoid locality, Zhaotong in Yunnan Province (Dong et al., 2014) from Shuitangba lignite beds (6.1–5.9 Ma), the terminal Miocene (Ji et al., 2013). It is roughly contemporary with *M. lacustris* and *M. nanus* from Yushe Basin in Shanxi Province (Teilhard de Chardin and Trassaert, 1937). The Early Pleistocene muntjaks are mainly those survived from the Neogene such as *M. nanus* and *M. lacustris*, and new members such as *M. bohlini* and *M. fenhoensis* (Chow, 1956) in northern China, as well as *M. hengduanshanensis* in southern China (Zong et al., 1996). The generic status of *M.* ?*huangi* from Yantouxi at Wushan (Dong and Chen, 2015) is not certain, otherwise it is another Early Pleistocene muntjak. *M. lacustris* ranged in northern, central and southern China, it is a widely distributed muntjak in the Early Pleistocene. On the contrary, *M. bohlini* ranged mostly in Palaeoarctic and transitional regions in China during the Early Pleistocene.

Cervavitus ranges mostly in the Neogene (Vislobokova, 1990), with two species *Cervavitus fenqii* (Han, 1987) and *C. ultimus* (Lin et al., 1978) survived to the Early Pleistocene. The pliocervine from Xinyaozi is larger than other Pleistocene ones such as *C. fenqii* and *C. ultimus* but relatively close to the Late Miocene *C. huadeensis* (Tables 5–6). If the taxonomic status of *Cervavitus* cf. *C. huadeensis* of Xinyaozi specimens can be confirmed, its chronological range could extend from the Late Miocene to the Early Pleistocene, and its geographic distribution from Nei Mongol southwards to Shanxi.

Axis originated in the Late Miocene and ranges to the present (Bai et al., 2017). *Axis shansius* appeared first in the Early Pliocene in Yushe Basin of North China (Teilhard de Chardin and Trassaert, 1937; Li et al., 1984; Tedford et al., 2013) and dispersed to Xihoudu (Chia and Wang, 1978) and Lantian (Chi, 1975) in North China, Tuozidong in East China (Dong and Fang, 2004), Yuanmou in South China (Lin et al., 1978) and Luotuoshan in Northeast China during the Early Pleistocene (Bai et al., 2017). It is therefore a common member of the Pleistocene mammalian faunas in China.

Nipponicervus elegans was first uncovered in Xiashagou locality in Nihewan Basin and it was placed in subgenus *Cervus* (*Rusa*) (Teilhard de Chardin and Piveteau, 1930). It was reported from Yushe (Teilhard de Chardin and Trassaert, 1937), Yangguo of Lantian (Chi, 1975) and Anping of Liaoyang (Zhang et al., 1980). It was reassigned to *Nipponicervus* (Qiu et al., 2004). Its chronological range is limited from the Early to Middle Pleistocene and its geographic range in northern and northeastern China.

The taxonomic status of red-deer-wapiti, or elaphoid group is quite complicated. They

were regarded as a subgenus *Cervus* (e.g. Nowak and Paradiso, 1983) or *Elaphus* (e.g. Wang and Wu, 1979). The group has many fossil and extant species or subspecies (e.g. Nowak and Paradiso, 1983; Sheng, 1992; Wang, 2003; Croitor and Obada, 2018; Croitor, in press). The first fossil red-deer-wapiti in China was described as *Cervus canadensis fossilis*, or *Cervus canadensis mongoliae* (Zdansky, 1925). It was revised later as *Cervus* (*Elaphus*) *canadensis* (Wang and Wu, 1979), and recently as *Cervus canadensis mongoliae* (Croitor, in press). The group in China was found mostly in northern regions such as Xujiayao (Hou et al., 2013), Salawusu (Qi, 1975; Hou et al., 2013), Shiyu (Jia et al., 1972), Upper Cave (Pei, 1940), Xiaogushan (Dong et al., 2010), Yanjiagang (Wei et al., 1986), etc. Morphology based taxonomy regarded European and Asian red deer (*Cervus elaphus elaphus*) and North American wapiti (*Cervus elaphus canadensis*) as two subspecies (e.g. Nowak and Paradiso, 1983; Sheng, 1992; Wang, 2003). It was supported by the fully fertile hybrids that can be produced under captive conditions (Moore and Littlejohn, 1989; Perez-Espona et al., 2013). But that based on molecular evidence place them in two separate species (Kuwayama and Ozawa, 2000; Pitra et al., 2004). And that based on both is very complicated (Groves and Grubb, 2011). The absence of bez tine is mostly seen in European red deer (Abbazzi, 1995; Baker et al., 2014). The Dazhuangke specimen is therefore included into the European red deer group as *Cervus* (*Elaphus*) *elaphus*. But the horizon of the Dazhuangke specimen is not yet certain. Because the most elaphoid specimens were uncovered from the Late Pleistocene deposits (Wang and Wu, 1979; Huang, 1991; Croitor, in press), some from the Middle Pleistocene (Abbazzi, 1995; Croitor, in press). On the other hand, Dazhuangke is about 2.8 km southwest of Taijiaping and 4.2 km southwest of Shuichongkou although it is in Xinyaozi Ravine. There is no other identified specimens can help to correlate the horizon. The described antler is the only identified specimen from Dazhuangke and it looks unlike those from the Early Pleistocene deposits at Shuichongkou and Taijiaping localities. It is therefore probably not contemporary with the Early Pleistocene deposits at Shuichongkou and Taijiaping localities, but not certain.

To conclude, total seven species of Cervidae were identified from the fossil specimens collected from Xinyaozi Ravine: *Muntiacus bohlini*, *Cervavitus* cf. *C. huadeensis*, *Axis shansius*, *Nipponicervus elegans*, *Elaphurus davidianus predavidianus*, *Elaphurus bifurcatus* and *Cervus* (*Elaphus*) *elaphus*. The previous six species with different body sizes and antler patterns are from the Early Pleistocene deposits at Taijiaping and Shuichongkou localities (with a chronological range of 2.6–1.7 Ma), and the last one from uncertain horizon at Dazhuangke. At least six species of cervids existed inside and around Sangganhe Basin during the Early Pleistocene. *C.* cf. *C. huadeensis* and *A. shansius* were survivors from the Late Neogene; *M. bohlini*, *N. elegans*, *E. davidianus predavidianus* and *E. bifurcatus* are new forms of the Early Pleistocene. If Dazhuangke horizon can be dated as those of Shuichongkou and Taijiaping, the appearance of elaphoid cervids could be traced back to the Early Pleistocene, and the evolution of elaphoid antler would start from the absence to the presence of bez tine. Cronin et al. (1994)

indicated that eight glacial events can be inferred between 2.7 and 2.3 Ma and the sea level dropped about 50–60 m in the Sea of Japan. The presence of the Early Pleistocene *Elaphurus* and *Nipponicervus* in mainland China (Teilhard de Chardin and Piveteau, 1930; Chi, 1975; Chia and Wang, 1978; Qiu et al., 2004; Dong et al., 2019) and Japanese archipelago (Otsuka, 1968, 1972; Otsuka and Hasegawa, 1976; Otsuka and Shikama, 1978) added new evidence that the sea level was dropped down that these cervids could migrate from the mainland to the islands. The abundance of folivorous cervid specimens in the Xinyaozi Ravine area implies the existence of a certain scale of forested environment in Sangganhe Basin area during the Early Pleistocene.

Acknowledgements The present work was supported by the Strategic Priority Research Program of Chinese Academy of Sciences, Grant No. XDB 26030304. The authors would like to acknowledge Professor Wei Qi for providing the material of the present study. They would also like to thank reviewers for comments and suggestions to improve the manuscript.

山西天镇辛窑子早更新世鹿科化石新材料

董　为[1,2]　白炜鹏[1,2,3]　潘　越[1,2,3]　刘文晖[4]

(1 中国科学院古脊椎动物与古人类研究所，中国科学院脊椎动物演化与人类起源重点实验室 北京 100044)

(2 中国科学院生物演化与环境卓越创新中心 北京 100044)

(3 中国科学院大学 北京 100049)

(4 中国国家博物馆环境考古研究所 北京 100006)

摘要：20世纪80年代在桑干河盆地一带考察泥河湾层时，在山西省天镇县南高崖乡的台家坪、水冲口和大庄科的辛窑子沟一带发现了很多哺乳动物化石地点并出土了很多哺乳动物化石。最近对其中鹿科化石的研究鉴定出7个种：步氏麂(*Muntiacus bohlini*)、化德祖鹿相似种(*Cervavitus* cf. *C. huadeensis*)、山西轴鹿(*Axis shansius*)、华丽日本鹿(*Nipponicervus elegans*)、始麋鹿(*Elaphurus davidianus predavidianus*)、双叉麋鹿(*E. bifurcatus*)及赤鹿(*Cervus* (*Elaphus*) *elaphus*)。其中前6个种产自台家坪和水冲口化石地点的泥河湾组中，层位相当于欧洲的中、晚维拉方期，即早更新世，而赤鹿产自大庄科化石地点，层位目前还不确定，但可能也是泥河湾组。因此在辛窑子沟一带的早更新世目前发现的鹿科化石至少有6个种。其中的化德祖鹿相似种和山西轴鹿是从晚新近纪残留下来的种类，而步氏麂、华丽日本鹿、始麋鹿和双叉麋鹿是早更新世出现的新种类。如果大庄科地点的层位可以确定为早更新世的话，赤鹿的最早记录则可以回溯到早更新世，其鹿角的演化是始于无冰枝，然后出现冰枝。另外，在中国大陆和日本列岛都发现过麋鹿和日本鹿化石，进一步说明在早更新世期间海平面曾经下降很多，使得大陆的一些鹿类得以迁徙到列岛上。最后，数量较多的低冠鹿科化石标本指示桑干河盆地一带在早更新世存在一定范围的森林环境。

关键词：山西天镇，辛窑子，桑干河盆地，泥河湾组，早更新世，中、晚维拉方期，鹿科

中图法分类号：Q915.876　　**文献标识码**：A　　**文章标号**：1000–3118(2020)03–0221–28

References

Abbazzi L, 1995. Occurrence of palmated *Cervus elaphus* from Italian Late Pleistocene localities. Rend Fis Acc Lincei, 6: 189–206

Azanza B, Rössner G E, Ortiz-Jaureguizar E, 2013. The early Turolian (Late Miocene) Cervidae (Artiodactyla, Mammalia) from the fossil site of Dorn-Dürkheim 1 (Germany) and implications on the origin of crown cervids. Palaeobio Palaeoenv, 93: 217–258

Bai W P, Dong W, Liu J Y et al., 2017. New material of *Axis shansius* (Mammalia, Artiodactyla) and phylogenetic consideration of *Axis*. Quat Sci, 37(4): 821–827

Bai W P, Dong W, Zhang L M et al., 2019. New material of the Early Pleistocene spiral horned antelope *Spirocerus* (Artiodactyla, Mammalia) from North China and discussion on its evolution. Quat Int, 522: 94–102

Baker K, Carden R, Madgwick R, 2014. Deer and People. Oxford: Windgather Press. 1–248

Chen G F, 2004. Artiodactyla. In: Zheng S H ed. Jianshi Hominid Site. Beijing: Science Press. 254–308

Chi H X, 1975. The Lower Pleistocene mammalian fossils of Lantian District, Shensi. Vert PalAsiat, 13(3): 169–177

Chia L P, Wang J, 1978. Hsihoutu–a Culture Site of Early Pleistocene in Shansi Province. Beijing: Cultural Relics Publishing House. 1–85

Chow M C, 1954. Villafranchian mammals from Tongshanzhen Basin, southern Shansi. Acta Palaeontol Sin, 2(3): 333–342

Chow M C, 1956. A new fossil muntjac from central Shansi. Acta Palaeontol Sin, 4(2): 229–232

Croitor R, 2019. A new form of wapiti *Cervus canadensis* Erxleben, 1777 (Cervidae, Mammalia) from the Late Pleistocene of France. Palaeoworld, doi:10.1016/j.palwor.2019.12.001

Croitor R, Obada T, 2018. On the presence of Late Pleistocene wapiti, *Cervus canadensis* Erxleben, 1777 (Cervidae, Mammalia) in the Palaeolithic site Climăuți II (Moldova). Contrib Zool, 87(1): 1–10

Cronin T M, Kitamura A, Ikeya N et al., 1994. Late Pliocene climate change 3.4–2.3 Ma: paleoceanographic record from the Yabuta Formation, Sea of Japan. Palaeogeogr, Palaeoclimatol, Palaeoecol, 108: 437–455

De Vos J, Mol D, Reumer J W, 1995. Early Pleistocene Cervidae (Mammalia, Artiodactyla) from the Oosterschelde (the Netherlands), with a revision of the cervid genus *Eucladoceros* Falconer, 1868. Deinsea, 2: 95–121

Dong W, 2004. The dental morphological characters and evolution of Cervidae. Acta Anthrop Sin, 23(Supp): 286–295

Dong W, 2006. Early Pleistocene ruminants (Mammals) from the Dajushan, Huainan, Anhui Province (China). Vert PalAsiat, 44(4): 332–346

Dong W, 2007. New material of Muntiacinae (Artiodactyla, Mammalia) from the Late Miocene of northeastern Qinghai-Tibetan Plateau, China. C R Palevol, 6(5): 335–343

Dong W, Chen S K, 2015. An extraordinary pattern of ruminant molars and associated cervids from the Pleistocene of Wushan, Central China. Vert PalAsiat, 51(3): 207–218

Dong W, Fang Y S, 2004. The Cervidae (Artiodactyla, Mammalia) from the Tuozidong at Tangshan, Jiangsu Province, China. Acta Anthrop Sin, 23(Supp): 296–305

Dong W, Hu C K, 1994. The Late Miocene Cervidae from Hounao, Yushe Basin, Shanxi. Vert PalAsiat, 32(3): 209–227

Dong W, Li Z Y, 2008. Late Pleistocene Artiodactyla (Mammalia) from the Lingjing Site, Xuchang, Henan Province (China). Vert PalAsiat, 46(1): 31–50

Dong W, Pan Y R, Liu J H, 2004. The earliest *Muntiacus* (Artiodactyla, Mammalia) from the Late Miocene of Yuanmou, southwestern China. C R Palevol, 3(5): 379–386

Dong W, Qiu Z X, Wang F Z, 2009. Artiodactyla. In: Jin C Z, Liu J Y eds. Paleolithic Site–The Renzidong Cave, Fanchang, Anhui Province. Beijing: Science Press. 321–335

Dong W, Fu R Y, Huang W W, 2010. Age and paleoenvironment of Xiaogushan fauna at Haicheng, Liaoning Province. Chinese Sci Bull, 55(24): 2704–2708

Dong W, Pan W S, Sun C K et al., 2011. Early Pleistocene ruminants from Sanhe Cave, Chongzuo, Guangxi, South China. Acta Anthrop Sin, 30(2): 192–205

Dong W, Ji X P, Nina G et al., 2014. New materials of the Late Miocene *Muntiacus* from Zhaotong hominoid site in southern China. Vert PalAsiat, 50(3): 316–327

Dong W, Liu W H, Zhang L M et al., 2018. New materials of Cervidae (Artiodactyla, Mammalia) from Tuchengzi of Huade, Nei Mongol, North China. Vert PalAsiat, 56(2): 157–175

Dong W, Wei Q, Bai W P et al., 2019. New material of the Early Pleistocene *Elaphurus* (Artiodactyla, Mammalia) from North China and discussion on taxonomy of *Elaphurus*. Quat Int, 519: 113–121

Gilbert C, Ropiquet A, Hassanin A, 2006. Mitochondrial and nuclear phylogenies of Cervidae (Mammalia, Ruminantia): systematics, morphology, and biogeography. Mol Phylogenet Evol, 40: 101–117

Groves C, Grubb P, 2011. Ungulate Taxonomy. Baltimore: The Johns Hopkins University Press. 1–310

Han D F, 1987. Artiodactyla fossils from Liucheng *Gigantopithecus* Cave in Guangxi. Mem Inst Vert Paleont Paleoanthrop, Acad Sin, 18: 135–208

Heintz E, 1970. Les Cervidés villafranchiens de France et d'Espagne. Mém Mus Natl Hist Nat, 22(1): 1–303

Hooijer, 1951. Two new deer from the Pleistocene of Wanhsien, Szechwan, China. Am Mus Novit, 1495: 1–18

Hou Y M, Yang S X, Dong W et al, 2013. Late Pleistocene representative sites in North China and their indication of evolutionary human behavior. Quat Int, 295: 183–190

Huang W B, 1991. The Late Pleistocene mammalian faunas of China. In: IVPP ed. Proceedings of the XIII International Quaternary Conference. Beijing: Beijing Scientific and Technological Publishing House. 44–54

Ji X P, Jablonski N G, Su D F et al., 2013. Juvenile hominoid cranium from the terminal Miocene of Yunnan, China. Chinese Sci Bull, 58(31): 3771–3779

Jia L P, Gai P, You Y Z, 1972. Reports on excavations at Shiyu Paleolithic site in Shanxi Province. Acta Archaeol Sin, 1: 39–58

Kuwayama R, Ozawa T, 2000. Phylogenetic relationships among european red deer, wapiti, and sika deer inferred from mitochondrial DNA sequences. Mol Phylogenet Evol, 15(1): 115–123

Li C K, Wu W Y, Qiu Z D, 1984. Chinese Neogene: subdivision and correlation. Vert PalAsiat, 22(3): 163–178

Lin Y P, Pan Y R, Lu Q W, 1978. The mammalian fauna of Early Pleistocene from Yuanmou, Yunnan. In: IVPP ed. Proceedings of Paleoanthropology of the Institute of Vertebrate Paleontology and Paleoanthropology, Chinese Academy of Sciences. Beijing: Science Press. 101–125

Liu P, Deng C L, Li S H et al., 2012. Magnetostratigraphic dating of the Xiashagou Fauna and implication for sequencing the mammalian faunas in the Nihewan Basin, North China. Palaeogeogr, Palaeoclimatol, Palaeocol, 315(5): 75–85

Moore G H, Littlejohn R P, 1989. Hybridisation of farmed wapiti (*Cervus elaphus manitobensis*) and red deer (*Cervus elaphus*). New Zeal J Zool, 16(2): 191–198

Nowak R M, Paradiso J L, 1983. Walker's Mammals of the World. Baltimore: The Johns Hopkins University Press.

1–1362

Otsuka H, 1968. A new species of *Elaphurus* from the Akaski Formation in Hyogo Prefecture, Japan. Rep Fac Sci, Kogoshima Univ, 1: 121–127

Otsuka H, 1972. *Elaphurus shikamai* Otsuka (Pleistocene cervid) from the Akaski Formation of the Osaka Group, Japan, with special reference to the genus *Elaphurus*. Bull Natl Sci Mus, 151: 197–210

Otsuka H, Hasegawa Y, 1976. On a new species of *Elaphurus* (Cervid, Mammal) from Akishima City, Tokyo. Bull Natl Sci Mus, Ser C (Geogl), 2: 139–143

Otsuka H, Shikama T, 1978. Fossil Cervidae from the Toú–kóu–shan Group in Taiwan. Rep Fac Sci, Kogoshima Univ, 11: 27–59

Pei W C, 1940. The Upper Cave Fauna of Choukoutien. Palaeont Sin, New Ser C, 10: 1–86

Perez-Espona S, Hall R J, Perez-Barberia F J et al., 2013. The impact of past introductions on an iconic and economically important species, the red deer of Scotland. J Hered, 104(1): 14–22

Pitra C, Fickel J, Meijaard E et al., 2004. Evolution and phylogeny of old world deer. Mol Phylogenet Evol, 33(3): 880–895

Qi G Q, 1975. Quaternary mammalian fossils from Salawusu River District, Nei Mongol. Vert PalAsiat, 13(4): 239–249

Qi G Q, Dong W, Zheng L et al., 2006. Taxonomy, age and environment status of the Yuanmou hominoids. Chinese Sci Bull, 51(6): 704–712

Qiu Z D, 1979. Some mammalian fossils from the Pliocene of Inner Mongolia and Gansu (Kansu). Vert PalAsiat, 17(3): 222–235

Qiu Z X, 2002. *Hesperotherium*–a new genus of the last Chalicotheres. Vert PalAsiat, 40(4): 317–325

Qiu Z X, Wei Q, Pei S W et al., 2002. Preliminary report on *Postschizotherium* (Mammalia: Hyarcoidea) material from Tianzhen, Shanxi, China. Vert PalAsiat, 40(2): 146–160

Qiu Z X, Deng T, Wang B Y, 2004. Early Pleistocene mammalian fauna from Longdan, Dongxiang, Gansu, China. Palaeont Sin, New Ser C, 27: 1–198

Schlosser M, 1924. Tertiary vertebrates from Mongolia. Palaeont Sin, Ser C, 1: 1–132

Sheng H L et al., 1992. The Deer in China. Shanghai: East China Normal University Press. 1–305

Tedford R H, Qiu Z X, Flynn L J, 2013. Late Cenozoic Yushe Basin, Shanxi Province, China: Geology and Fossil Mammals. New York: Springer. 1–109

Teilhard de Chardin P, 1940. The fossils from locality 18 near Peking. Palaeont Sin, New Ser C, 9: 1–100

Teilhard de Chardin P, Piveteau J, 1930. Les mammifères fossils de Nihowan (Chine). Ann Paléont, 19: 1–134

Teilhard de Chardin P, Trassaert M, 1937. Pliocene Camelidae, Giraffidae and Cervidae of S. E. Shansi. Palaeont Sin, New Ser C, 1: 1–56

Tong H W, Tang Y J, Yuan B Y, 2011. Biostratigraphy division of vertebrate fossils. In: Yuan B Y, Xia Z K, Niu P S eds. Nihewan Rift and Ancient Human. Beijing: Geological Publishing House. 47–60

Vislobokova I A, 1990. The Fossil Deer of Eurasia. Moscow: Sciences Press. 1–208

Wang B Y, Wu W Y, 1979. The artiodactyla. In: IVPP ed. Vertebrate Fossils of China. Beijing: Science Press. 501–620

Wang S Q, 2014. New findings of ungulate teeth from the Early Pleitocene Longdan Fauna, China. In: Dong W ed. Proceedings of the 14th Annual Meeting of the Chinese Society of Vertebrate Paleontology. Beijing: China Ocean

Press. 37–46

Wang Y X, 2003. A Complete Checklist of Mammal Species and Subspecies in China–A Taxonomic and Geographic Reference. Beijing: China Forestry Publishing House. 1–394

Wei Q, 1997. The framework of archaeological geology of the Nihewan Basin. In: Tong Y S, Zhang Y Y, Wu W Y et al. eds. Evidence for Evolution–Essays in Honor of Prof. Chungchien Young on the Hundredth Anniversary of His Birth. Beijing: China Ocean Press. 193–207

Wei Z Y, Yang D S, Yin K P et al., 1986. Excavation report (1982–1983) of the Paleolithic site of Yanjiagang, Haerbin, China. North Cult Relics, 4: 7–15

Woodburne M O, Tedford R H, Lindsay E H, 2013. North China Neogene biochronology–A Chinese standard. In: Wang X M, Flynn L J, Fortelius M eds. Fossil Mammals of Asia–Neogene Biostratigraphy and Chronology. New York: Colombia University Press. 91–118

Xue X X, 1959. Cervidae. In: IVPP ed. Pleistocene Mammalian Fossils from the Northeastern Provinces. Beijing: Sciences Press. 52–60

Zdansky O, 1925. Fossile Hirsche Chinas. Palaeont Sin, Ser C, 2: 1–94

Zhang Z H, Zou B K, Zhang L K, 1980. The discovery of fossil mammals at Anping, Liaoyang. Vert PalAsiat, 18(2): 154–162

Zong G F, Chen W Y, Huang X S et al., 1996. Cenozoic Mammals and Environment of Hengduan Mountains Region. Beijing: China Ocean Press. 1–279